Available online at www.sciencedirect.com
SCIENCE DIRECT®

Journal of the European Ceramic Society 24 (2004) 2149–2156
www.elsevier.com/locate/jeurceramsoc

Fabrication and characterisation of silicon carbide/superalloy interfaces

Junqin Li[a], Ping Xiao[b,*]

[a]Department of Materials Science and Engineering, Shenzhen University, Shenzhen, GD518060, China and Department of Materials Engineering, Brunel University, Uxbridge UB8 3PH, UK
[b]Manchester Materials Science Centre, University of Manchester, Manchester M1 7HS, UK and Department of Materials Engineering, Brunel University UB8 3PH, UK

Received 13 January 2003; accepted 2 May 2003

Abstract

Both silicon carbide ceramic (sintered SiC or reaction-bonded Si-SiC) and Inconel 600 superalloy ($Ni_{72}Cr_{16}Fe_8$ in wt.%) are promising structural materials for high temperature application because of their excellent mechanical properties and good high temperature corrosion resistance. In this study, the reaction-bond silicon carbide (RBSC) was joined to an Inconel 600 ($Ni_{72}Cr_{16}Fe_8$ in wt.%) superalloy using the diffusion bonding method at temperatures from 900 to 1080 °C. The interfacial reaction between the RBSC and superalloy was investigated using optical and scanning electron microscopy (SEM), coupled with energy dispersive X-ray analysis (EDX) and wavelength dispersive spectroscopy (WDS). The reaction products were also studied using X-ray diffraction technique. The mechanical properties of the joints were examined using shear testing. Experimental results showed that the interfacial reaction products at 900 and 950 °C were various silicides with some voids formed in the RBSC. As the bonding temperature increased to 1000 °C, the superalloy/RBSC reactions become more intensive, although some pores in the RBSC were filled by the reaction products. With the bonding temperature increasing to 1080 °C, a thin layer of $CrSi_2$ was formed at superalloy/SiC interface without formation of any pores in the RBSC. The shear strength of this joint was measured as 126 MPa.

Keywords: Inconel 600; Interfaces; Joining; Reaction-bonded SiC; SiC

1. Introduction

Silicon carbide (sintered SiC or reaction-bonded SiC) is one of those promising structural electrical heating materials for high temperature applications because of its excellent mechanical properties and resistance to high temperature corrosion. However, because of difficulties in producing large and complex shape ceramic components, it is necessary to join SiC to itself and/or to metals for the construction of a ceramic component of required shape and reduce cost. At present, two joining techniques, brazing with metallic alloy and solid state diffusion bonding, are receiving increasing attention for the construction of ceramic components.[1,2]

Designing and controlling the chemical reactions between SiC and metals is an important issue in the fabrication of the SiC/metal joints. Formation of various reaction products at the SiC/metal interface during the joining process may lead completely different mechanical properties of the joints. In some cases, the reactions between the brazing alloy and SiC led to the formation of porosity and brittle compounds at the interface of the joint,[3,4] where the joint was weakened. On the other hand, the formation of chemical bonds at the metal/ceramic interface is essential for producing a strong metal/ceramic joint. McDermid et al.[4] used solution thermodynamic theory to compute an optimum composition of Ni–Cr–Si alloy for brazing SiC ceramic. They pointed out that the alloys containing less Si lead to the formation of a porous reaction zone at the brazing alloy/SiC interface due to the excessively vigorous joining reaction between brazing alloy and ceramic. Too high Si content alloys exhibited debonding of the

* Corresponding author. Tel.: +44-161-200-5941; fax: +44-161-200-3586.
E-mail address: ping.xiao@man.ac.uk (P. Xiao).

0955-2219/03/$ - see front matter © 2003 Elsevier Ltd. All rights reserved.
doi:10.1016/S0955-2219(03)00369-8

brazing alloy from the SiC. The reactions between SiC and metals, e.g. Ti,[5] Ni, Cr,[6] Ta,[7] Nb,[8] Mo,[9] Ni–Cr alloy[10] or TiAl-based alloy,[2] have been studied extensively. However, most of these metals are too active at high temperature and their oxidation resistance is poor for high temperature applications. Inconel 600 superalloy ($Ni_{72}Cr_{16}Fe_8$ in wt.%) has high temperature strength and very good resistance to high temperature oxidation. Fabrication of the SiC/superalloy interfaces may lead to the production of the SiC/metal joints, which can be used at high temperature environments. McDermid et al.[11] fabricated the SiC-Inconel 600 superalloy joint using Fe-based alloy and analysed the phases formed at the interfaces of the joint. To our knowledge, there has been no report on the study of the interfacial reactions between reaction-bonded SiC (RBSC) and Inconel 600 superalloy. In this work, we have examined the chemical reactions that occurred at the RBSC/Inconel 600 interface between 900 °C and 1080 °C, and related the microstructure of the interfaces to the mechanical behaviour of the joints.

2. Experiment procedure

The RBSC was supplied by the Pi Kem Ltd, UK. Microanalysis showed that the RBSC contained 9.6 vol.% free Si. Inconel 600 superalloy foils, supplied by the Goodfellow Ltd, U.K, are 0.2 mm thick with a nominal composition of Ni–15.5% Cr–8% Fe (in wt.%).

The RBSC cylindrical bar with the diameter of 12 mm was cut into plates with the thickness of 4.0 mm. The flat surface of the SiC was polished using diamond paste with the final grit size of 6 μm. Both RBSC and Inconel 600 foils were ultrasonically cleaned in acetone prior to joining. The RBSC/alloy foil/RBSC sandwich was placed in a graphite sample holder to keep the ceramics and the alloy aligned throughout the joining process. The joints were performed in vacuum of 5×10^{-5} torr between 900 °C and 1080 °C with applied pressure of 2.2 MPa for 30 min. The heating rate and cooling rate are 10 and 5 °C/min, respectively.

After joining, the RBSC/alloy foil/RBSC joints were cross-sectioned using a diamond saw, then polished with diamond paste to a 1 μm finish, followed by ultrasonic cleaning in acetone. The cross-section of the joints was characterised using optical and scanning electron microscopy (SEM) coupled with energy dispersive X-ray microanalysis (EDX) and wavelength dispersive spectroscopy (WDS) (Jeol JXA-840). For each phase, three to five analyses were made using EDX and WDS to obtain the average value of the composition. In order to verify the phases formed in the reaction layers of the joint during joining, the alloys with the composition obtained by EDX for each phase was prepared by powder metallurgy method using the same heat treatment as that in joining. The phase of the alloys were identified by XRD (Philip PW140/00) analysis. The samples with the size of $5.0\times8.0\times10.0$ mm were cut for the shear testing. The shear strength of the joints fabricated at 1000 and 1080 °C was measured at room temperature. The shear strength results are the average of two tests for each joining condition.

3. Results

3.1. Microstructures and phase analysis of the joints

Fig. 1 shows microstructure of the cross-section of the RBSC/Inconel 600 joints fabricated at 900, 950, 1000 and 1080 °C for 30 min, respectively. The microstructure and phase composition of the reaction layers depends on the fabrication temperatures. Three reaction layers, labelled as A, B and C, were produced between the RBSC and the superalloy at 900 and 950 °C (Fig. 1 a and b). These reaction layers produced at 950 °C are thicker than those produced at 900 °C. In both cases, some residual superalloy was left in the middle of the joint. The thickness of the residual superalloy is 180 μm for the joint fabricated at 900 °C while 35 μm in the joint fabricated at 950 °C. For the joint fabricated at 1000 °C, there was no superalloy left after joining such that three reaction layers, labelled as A′, B′ and C′ were found in this joint (Fig. 1c). In the joint fabricated at 1080 °C, only one thin reaction layer was found after the joining (Fig. 1d).

The concentrations of Ni, Cr, Fe and Si in the reaction layers were determined using EDX while the distribution of carbon in the reaction layers was obtained from the WDS line scan. The phases of each reaction layer was determined using the XRD analysis of the reaction product, which was prepared from the powder mixture with the same composition as the reaction product in the joint and was exposed to the same thermal treatment as the joint experienced. Figs. 2(a) and 3 show the SEM microstructure and the concentration profile of carbon obtained from the WDS line scan across the joint (along the dark line) of the reaction layers in the joint, which was produced at 950 °C. Table 1 gives the compositions and phases of the reaction layers produced at 950 °C. The A, B and C layers in Fig. 3 correspond to the A, B and C layers in Fig. 2(a), respectively. Because the superalloy has very low solubility of carbon, the region showing the lowest carbon content should be free of carbon. Two large peaks of the carbon line in the B and C layer correspond to the SiC region (dark phase). The WDS scan also shows that carbon is present in the needle-like dark grey region in grey matrix of layer A, grey region of layer B and grey matrix of layer C, and existed in dark grey region of layer B. It is reasonable to assume that the needle-like

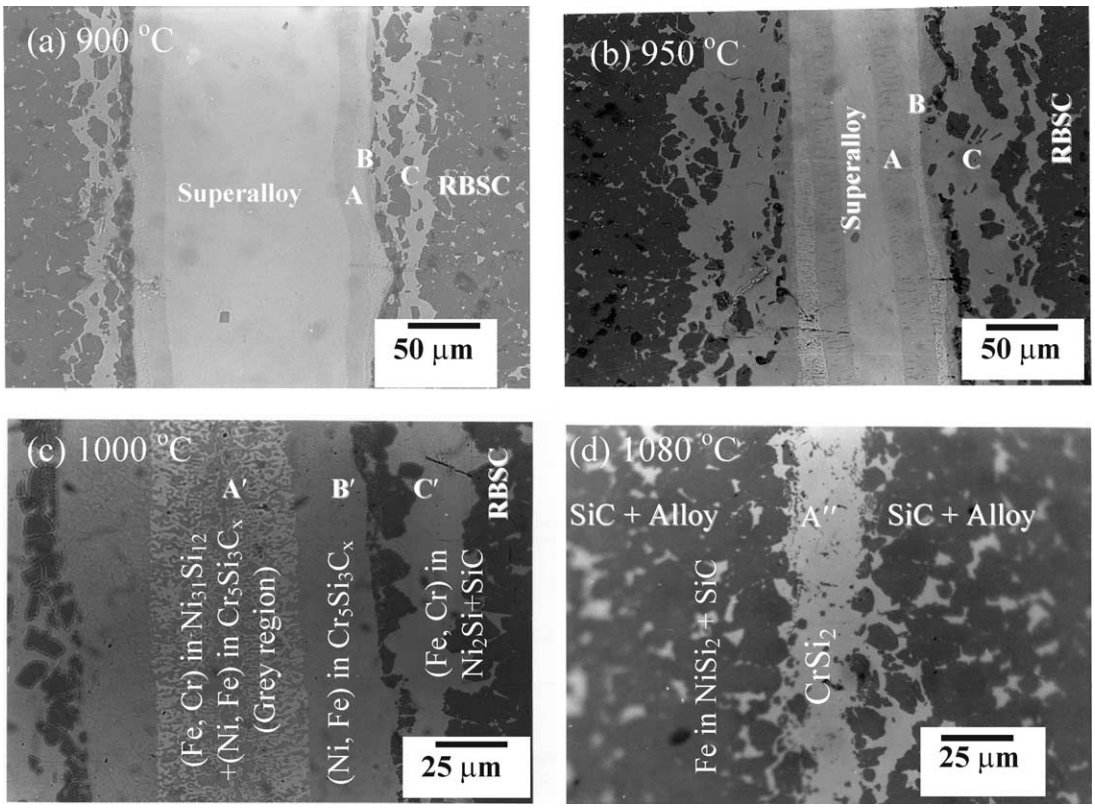

Fig. 1. Optical images showing the cross-section of the RBSC/Inconel 600 joints produced at (a) 900 °C, (b) 950 °C, (c) 1000 °C (d) 1080 °C for 30 min.

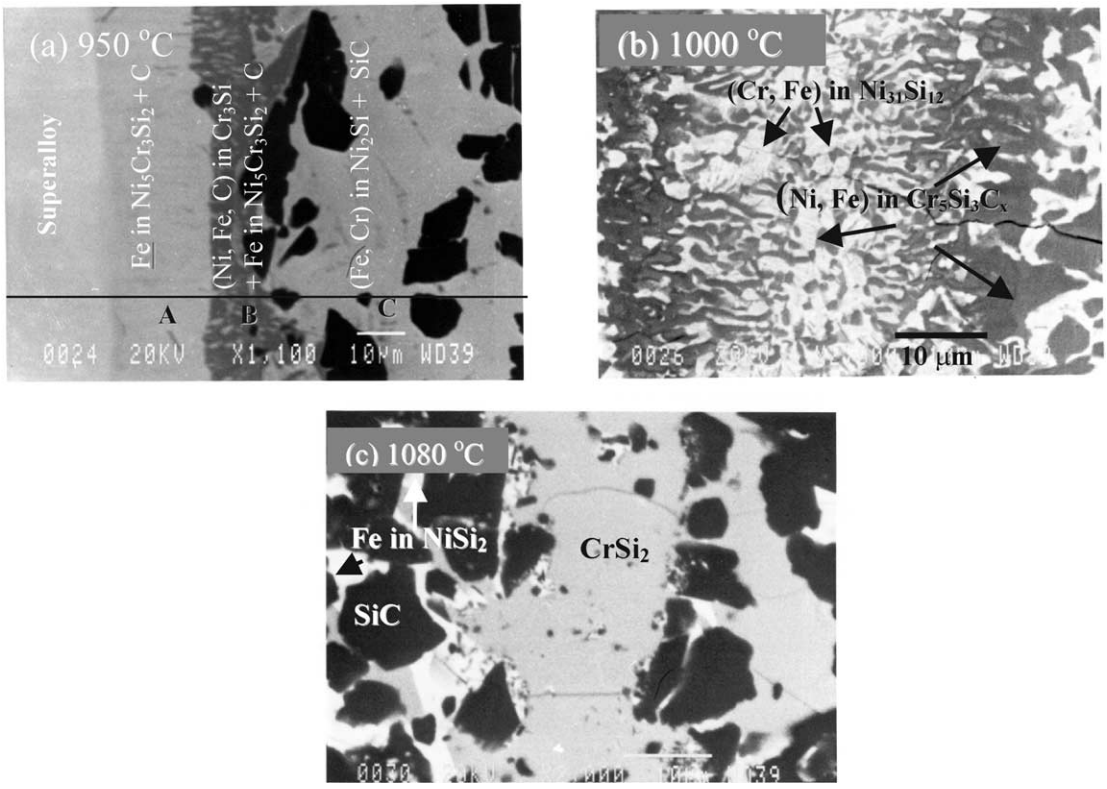

Fig. 2. SEM micrographs showing the detailed microstructures of the joints produced at (a) 950 °C, (b) 1000 °C (c) 1080 °C for 30 min.

carbon phase, not in solution, is present in the matrix of layers A, in grey region of layer B and in the matrix of layer C. Fig. 4 shows the XRD patterns of the product with the same compositions as that in the matrix phase in layer A, the matrix phase (dark grey region) and the dispersive phase (light grey region) of layer B respectively (see Table 1). The XRD pattern of the product corresponding to the matrix phase with composition of 45.2Ni–25.0Cr–19.3Si–10.6Fe (in at.%) in layer A mainly shows the XRD peaks of $Ni_5Cr_3Si_2$ with small amount of pure Ni (unreacted). This indicates that some or most of 10.6% Fe dissolved in $Ni_5Cr_3Si_2$ during the joining. Therefore, the matrix phase in layer A should be a solid solution of Fe in $Ni_5Cr_3Si_2$. Simlarly, the XRD pattern corresponding to the matrix phase (dark grey region) in layer B with composition of 2.9Ni–68.9Cr–24.7Si–3.5Fe shows the XRD peaks of a Cr_3Si phase (Fig. 4b). The carbon was detected in this phase by WDS line scan in this work (Fig. 3). The solubility of carbon in Cr_3Si was reported to be around 4 at.%.[12] Therefore, this matrix phase should be a solid solution of (Fe, Ni, C) in Cr_3Si. The XRD pattern corresponding to the dispersive light grey phase in the layer B shows the mixed patterns of solid solutions of Fe in $Ni_5Cr_3Si_2$ and (Fe, Ni, C) in Cr_3Si (Fig. 4c), so this dispersive light grey phase in the layer B should be a solid solution of Fe in $Ni_5Cr_3Si_2$, which is the same matrix phase as in the layer A. It should be noted that the composition of this phase obtained by EDX may affected by the matrix phase due to its fine structure. The XRD pattern corresponding to the matrix phase in the layer C shows Ni_2Si phase (Fig. 4d), including high temperature structure θ-Ni_2Si and low temperature structures δ-Ni_2Si, so it is a solid solution of Fe and Cr in Ni_2Si. The dark phase in the layer C was identified as SiC. Therefore, the layer C contains a solid solution of (Fe, Cr) in Ni_2Si and SiC. Microanalysis also showed the presence of NiSi containing

Table 1
Phase compositions (at.%) in the reaction layers formed at 950 °C for 30 min

Layer and region	Ni	Cr	Si	Fe	Phases
Central layer	72.0	18.5	0	9.5	α-(Ni, Cr, Fe)
Layer A	45.2	25.0	19.3	10.6	Fe in $Ni_5Cr_3Si_2$ + C
Layer B (dark region)	2.9	68.9	24.7	3.5	(Fe, Ni, C) in Cr_3Si
Layer B (grey region)	39.5	32.2	24.8	3.5	Fe in $Ni_5Cr_3Si_2$ + C
Layer C (grey phase)	56.1	4.2	32.6	7.1	(Fe, Cr) in Ni_2Si

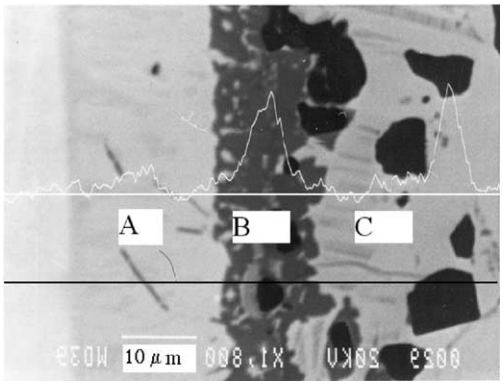

Fig. 3. A microanalysis line scan showing the distribution of carbon along the dark marked line in the reaction zone produced at 950 °C. The left side is the superalloy, while A, B and C have the same compositions as shown in Fig. 2a.

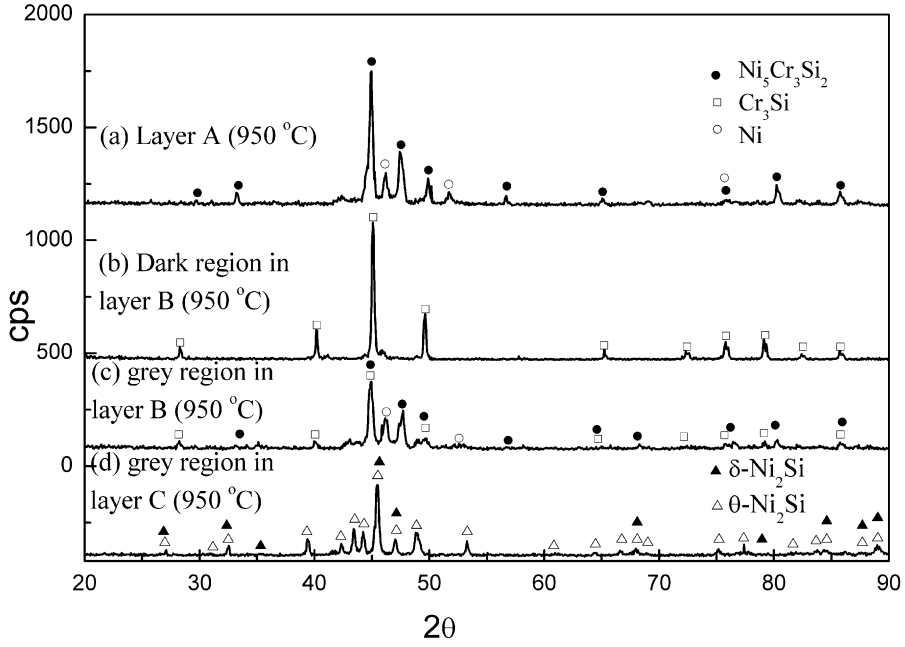

Fig. 4. XRD patterns for the alloys with compositions (shown in Table 1) matrix phase in layer A (a), dark grey region (b), light grey region (c), of layer B and matrix phase in layer C (d), shown in Fig. 2(b), for the joint fabricated at 950 °C.

a small amount of Fe but very little of Cr, which replace the original Si network within the RBSC region of about 900 μm away from the layer C. This suggests that Ni with some Fe from the superalloy diffused into the Si channels and formed Ni–Si solid solution in the RBSC. The phases existed in the reaction layers for this joint are labelled in Fig. 2(a) and listed in Table 1.

In the same way, the phases formed in the reaction layers in the joints fabricated at 1000 °C were verified. Based on the EDX results given in Table 2 and XRD patterns of the corresponding products shown in Fig. 5, the reaction layers shown in Fig. 1c are given in Table 2. In the joint fabricated at 1080 °C, only one reaction layer was formed between the two SiC substrates (Fig. 1d). Microanalysis results, given in Table 3, indicate that the layer is $CrSi_2$, labelled in Fig. 2c. All of the Si network in the RBSC substrate was replaced by the nickel silicide ($NiSi_2$). Almost no Cr was found in the RBSC after the joining. Carbon may be present due to decomposition of some SiC, but carbon content may be too low to be detected.

Some pores in the RBSC were found close to the reaction layers in the joints and their distribution depends on the fabrication temperatures. Fig. 6(a)–(d) show the pores in the RBSC close to the reaction layers for the joints fabricated at 900, 950, 1000 and 1080 °C, respectively. Image analysis showed that the average volume fraction of the pores in RBSC is 10.8 vol.%, very close to that of the Si in RBSC before the joining (9.6 vol.%). The pores region in the RBSC is about 300 μm deep from the reaction layers in the joint fabricated at 900 °C (Fig. 6a), and is about 800 μm deep in the joint produced at 950 °C (Fig. 6b). However, at 1000 °C, the pores region is 200 μm deep (Fig. 6c), and no pores appeared in the RBSC beside the reaction layers. It seems that some voids were filled with some reaction product phase during the joining. EDX analysis showed that this reaction product phase is NiSi phase. Almost no pores were found in the joint fabricated at 1080 °C (Fig. 6d).

3.2. Shear strength

The shear test was performed on the RBSC/Inconel 600/RBSC joints fabricated at 1000 and 1080 °C. The plots of shear stress versus cross-head displacement for

Table 2
Phase compositions (at.%) in the reaction layers formed at 1000 °C for 30 min

Layer and region	Ni	Cr	Si	Fe	Phases
Layer A′ (white region)	45.7	10.3	31.0	11.8	(Cr, Fe) in $Ni_{31}Si_{12}$
Layer A′ (grey region)	5.0	51.3	36.8	6.9	(Ni, Fe) in $Cr_5Si_3C_x$
Layer B′	8.2	46.5	36.6	7.9	(Ni, Fe) in $Cr_5Si_3C_x$
Layer C′	59.2	3.3	31.5	6.0	(Fe, Cr) in Ni_2Si
Bright phase in RBSC matrix (near the reaction layer)	50.0	0.2	49.1	0.6	NiSi
Bright phase in RBSC matrix (far from the reaction layer)	27.1	0.3	66.8	5.9	Fe in $NiSi_2$

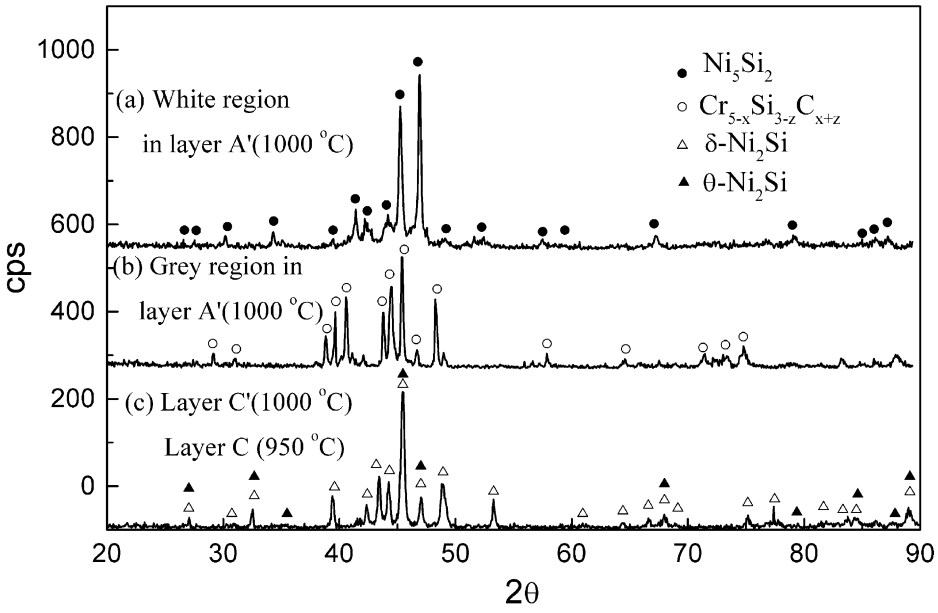

Fig. 5. XRD patterns for the alloys with compositions (shown in Table 2) of white region (a) and grey region (b) of layer A′ and layer C′ (layer C at 950 °C) (c), shown in Fig. 2(c), for the joint fabricated at 1000 °C.

Table 3
Phase compositions (at.%) in the reaction layers formed at 1080 °C for 30 min

Layer and region	Ni	Cr	Si	Fe	Phases
Central layer (layer A″)	0.9	33.7	65.1	0.3	$CrSi_2$
Bright phase in RBSC	30.7	1.3	65.5	2.5	(Fe, Cr) in $NiSi_2$

the two joints are shown in Fig. 7. For the joint fabricated at 1000 °C, the average shear strength for this joint is 56.0 MPa. The failure occurred within the reaction zones. For the joint fabricated at 1080 °C, the average shear strength is 126.0 MPa, while the failure occurred within the RBSC substrate. The presence of the pores, microcracks and complex interface structures in the joints fabricated at 900, 950 and 1000 °C should weaken the joint strength, whereas a dense and single layer joint fabricated at 1080 °C leads to strong bonding at the interfaces. The shear strength of the SiC/TiC/SiC joint reported by Menager et al.[13] was about 15 MPa where the joint was fabricated at 1200 °C. The shear strength increased to about 35 MPa when the joint was fabricated at 1400 °C. Naka et al.[14] also reported that the maximum shear strength for the SiC/V/SiC joints was 130 MPa at room temperature. In this work, the SiC/metal joints with high strength were produced by using a simple direct bonding technique. Such joints have a potential to be used at high temperature.

4. Discussion

The formation of the interfacial reaction layers at the joints are controlled by the joining temperature. The distribution of silicide phases and formation of large areas of pores in the interfacial regions suggests possible presence of a transient liquid phases during joining. For joining at 950 °C, the Inconel 600 reacted with the silicon present in the RBSC first, forming a liquid Ni–Si–Fe–Cr alloy, which proceeded into the RBSC via the Si network channels. This liquid also reacted with the SiC in the RBSC to produce silicides and C until the thermodynamics were unfavourable. The two reaction layers (A, B in Fig. 1a) beside the superalloy were formed through solid diffusion whereas the reaction layer (C) beside the RBSC seemed to be formed by solidification of a liquid Ni–Cr-Fe-Si alloy. For joining at 1000 °C, a Ni-rich Ni–Si–Fe–Cr liquid alloy was also formed and reacted with the RBSC. However, Cr was difficult to diffuse through the liquid alloy. As result, the high concentration of Cr from complete dissolution of the superalloy promoted formation of chromium silicides at the interface. It seemed that C′ layer (Fig. 1b) was formed from solidification of liquid alloys whereas the A′ and B′ layers was formed through solid diffusion. At 1080 °C, the reaction involved the formation of a single layer of chromium silicide at the interface and the formation of nickel silicides in the original Si channels without formation of pores. A previous study on reac-

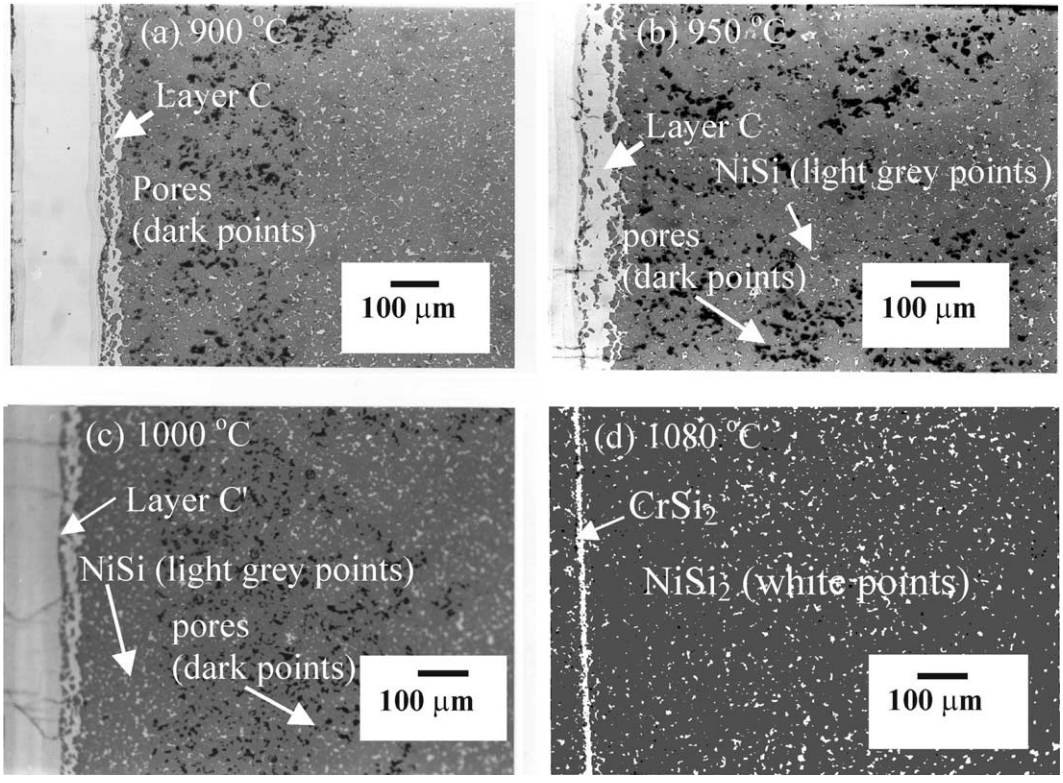

Fig. 6. Optical images showing the pores in the joints formed at (a) 900 °C (b) 950 °C, (c) 1000 °C (d) 1080 °C for 30 min.

tion between the $Ni_{82}Cr_{18}$ alloy and the RBSC at 950 °C for 16 h[10] showed the formation of $Ni_5Cr_3Si_{1.8}C$, Ni_5Si_2 containing dissolved Cr and Ni_2Si containing Cr and C. The reaction layers in the joint fabricated at 950 °C in this work (Fig. 2a) show much more complicated microstructure and phase compositions, which should be mainly caused by the presence of Fe in the superalloy and shorter joining time.

The formation and distribution of the pores were controlled by the diffusion of Si and the formation of Ni_2Si from the reaction between Si and Ni. For the joints fabricated at 900 and 950 °C, the Si in the region near the Inconel 600/RBSC interface in the RBSC diffused to react with Ni and formed the Ni_2Si phase, but the Si in the region far from the interface could not diffuse fast enough to compensate the loss of the Si caused by the reaction. At 1000 °C both NiSi and Ni_2Si were formed at the joining temperature. According to the Ni–Si phase diagram[15], NiSi should be a liquid phase at 992 °C, filling the space originally occupied by Si. Therefore, there are no pores in the region near the reaction layers, but some pores still exists in the region further away from the reaction layers as some Si diffused away to form nickel silicides. At 1080 °C, a liquid Ni–Si alloy was formed with dissolution of all the Si in the RBSC. The $NiSi_2$ phase was then formed from the

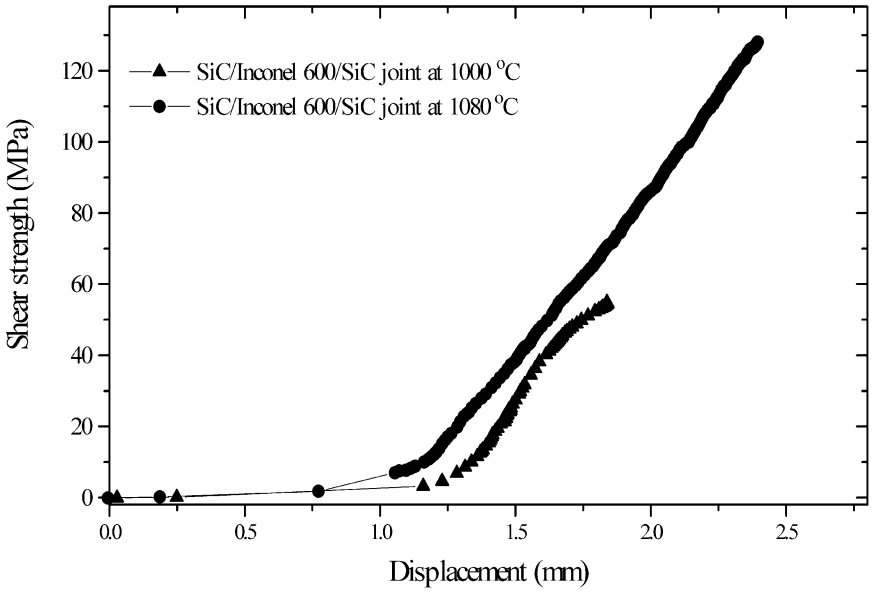

Fig. 7. Shear stress versus crosshead displacement for the joints produced at (a) 1000 °C (d) 1080 °C for 30 min.

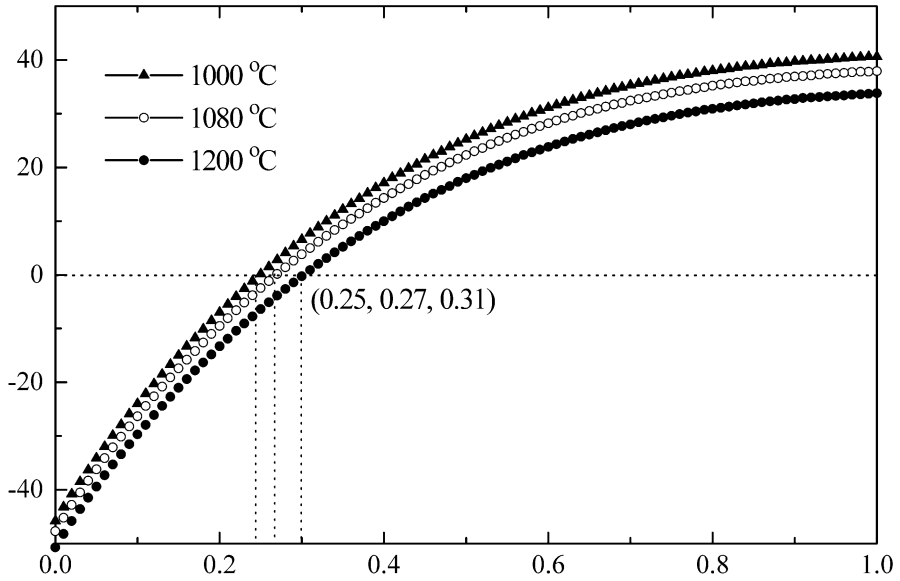

Fig. 8. Gibbs free energy change versus X_{Si} for the reaction between the liquid Ni–Si alloy and SiC.

solidification of the liquid Ni–Si alloy. No reaction between the liquid and SiC took place since the Si content was high enough to prevent the dissolution of SiC in the liquid Ni–Si alloy. No pores were formed since the nickel silicides replaced all of the Si in the RBSC. Image analysis showed that the volume fraction of $NiSi_2$ in RBSC is 10.2 vol.%, where very close to that of the Si in RBSC before the joining (9.6 vol.%).

The reaction between a liquid Ni–Si alloy and SiC depends on the Si content in the liquid alloy. Thermodynamic calculation of the reaction between Ni–Si and SiC would help us to understand the formation of nickel silicides in the porous SiC. It should be noted that the formation of complex compounds in the joints was confirmed by the XRD analysis, not by this thermodynamic calculation. Fig. 8 shows the Gibbs free energy change for the reaction between SiC and nickel silicides per mol SiC at 1000, 1080 and 1200 °C, respectively:

$$[Ni_xSi_{1-x}] + < SiC > = [Ni_xSi_{1-x}] + C$$

where x is the mol fraction of Ni in the Ni–Si liquid solution.

The Gibbs energy change ΔG for this reaction was calculated using the data obtained from ref 16. Fig. 8 shows that ΔG at 1000 °C is positive when $X_{Si} > 0.25$, indicating that at 1000 °C SiC is stable with the Ni–Si alloy when the alloy contains more than 25 at.% Si. Experimental results show that no reaction occurred between SiC and the NiSi phase at 1000 °C where the silicon content is about 50 at.% (Fig. 6c). However, reactions occurred between SiC and Ni to form Ni_2Si when the Si content was not high (Fig. 1c). At 1080 °C, the reaction products are $CrSi_2$ and a Ni–Si liquid alloy with the Si content higher than the equilibrium composition of 27% with SiC. Therefore, there was no significant dissolution of SiC into the liquid phase during the joining at 1080 °C. (Fig. 6d). For joining at 1080 °C, reactions mainly took place between the Inconel 600 superalloy and the free Si in the RBSC. No excessive brittle silicides were formed in the joints. Therefore, a strong bond was achieved between the two SiC pieces.

5. Conclusion

The joining and reactions between a reaction-bond silicon carbide (RBSC) and Inconel 600 superalloy at different temperature has been studied. The microstructure and composition of the RBSC/Inconel 600/RBSC joints depend on the fabrication temperature. The Si and/or SiC in the RBSC reacted with the Ni, Cr and Fe from the Inconel 600 to form various silicides, controlled by the diffusion and liquid alloy formation. The reaction products are mainly Ni- or Cr-based silicides with dissolved Fe. As the reaction layers were formed during the joining at lower temperature (1000 °C or lower), diffusion of the Si led to the formation of pores in the RBSC. At higher temperature (1080 °C) the formation of liquid Ni–Si alloy and precipitation of solid phases eliminated the formation of pores in the RBSC, leading to the formation of strong joints. Thermodynamic analysis indicated that both the joining temperature and the content of Si in the reaction layers was critical in controlling the reaction processes that occurred at the SiC/alloy interfaces.

References

1. Bhanumurthy, K. and Schmid-Fetzer, R., *Mater. Sci. Eng. A*, 1996, **220**, 35.
2. Liu, H. J., Feng, J. C. and Qian, Y. Y., *Scripta Mater.*, 2000, **43**, 49.
3. Boadi, J. K., Yano, T. and Iseki, T., *J. Mater. Sci.*, 1987, **22**, 2341.
4. McDermid, J. R. and Drew, R. A. L., *J. Am. Cerm. Soc.*, 1991, **74**(8), 1855.
5. Naka, M., Feng, J. C. and Schuster, J. C., *Met. Mater. Trans. A*, 1997, **28**, 1385.
6. Park, J. S., Landry, K. and Perepezko, J. H., *Mater. Sci. Eng. A*, 1996, **259**, 279.
7. Feng, J. C., Naka, M. and Schuster, J. C., *J. Mater. Sci. Lett.*, 1997, **16**, 1116.
8. Feng, J. C., Liu, H. J. and Li, Z. R., *Trans. Chin. Weld. Inst.*, 1997, **2**, 20.
9. Martinelli, A. E. and Drew, R. A. L., *Mater. Sci. Eng. A*, 1995, **191**, 239.
10. Backhaus-Ricoult, M., *Acta Metall. Mater.*, 1992, **40** (suppl.), s95.
11. McDermid, J. R. and Drew, R. A. L., *J. Mater. Sci.*, 1990, **25**, 4804.
12. Feng, J. C., Nata, M. and Schuster, J. C., *J. Jpn. Inst. Met*, 1997, **61**, 636.
13. C. H. Henager Jr., *Ceramic Joining*, Am. Ceram. Soc., OH, USA, p. 117.
14. Fukai, T., Naka, M., Feng, J. C. and Shuster, J. C., *J. Jan. I. Met*, 1998, **62**, 899.
15. Smithells, C. J., *Metals Reference Book,* 5th ed. Butterworth & Co Ltd, London, 1976.
16. Kaufman, L., *Calphad*, 1979, **3**(1), 45.